Molecular Neurobiology (2019) 56:4072–4085
https://doi.org/10.1007/s12035-018-1358-4

Upregulation of MicroRNA miR-9 Is Associated with Microcephaly and Zika Virus Infection in Mice

Haijun Zhang[1] · Yafei Chang[2] · Longbin Zhang[3] · Seung-Nam Kim[1,4] · Gaizka Otaegi[1] · Zhen Zhang[2] · Yanzhen Nie[2] · Taufif Mubarak[1] · Cui Li[5] · Cheng-Feng Qin[6] · Zhiheng Xu[5] · Tao Sun[1,3]

Received: 9 February 2018 / Accepted: 19 September 2018 / Published online: 27 September 2018

Abstract

Proper growth of the mammalian cerebral cortex, which is determined by expansion and survival of neural progenitors and mature neurons, is crucial for cognitive functions. Here, we show a role of the dosage of microRNA miR-9 in controlling brain size. Cortical-specific upregulation of miR-9 causes microcephalic defects in mice, due to apoptosis, reduced neural progenitor pool, and decreased neurogenesis. Glial cell-derived neurotrophic factor (GDNF) is a target of miR-9, and protects neural progenitors from miR-9-induced apoptosis. Furthermore, Zika virus (ZIKV) infection in embryonic mouse cortex causes reduced numbers in neural progenitors and newborn neurons, and results in upregulation of miR-9, downregulation of its target GDNF. Our studies indicate an association of altered levels of miR-9 and its target GDNF with microcephaly and ZIKV infection in mice.

Keywords Cerebral cortex · Neural progenitor · Apoptosis · miR-9 · GDNF · Zika virus

Introduction

Microcephaly is a neonatal brain malformation defined as small brain in size [1]. During normal cortical development, a fraction of neural progenitors and mature neurons undergoes apoptosis. Altering expression levels of genes that regulate cell survival and programmed cell death affects cortical size. For example, *EphA7* knockout mice display enlarged cortex due to reduced apoptosis [2]. Glial cell-derived neurotrophic factor (GDNF) has been proven to play a crucial protective role against neuronal apoptosis under normal and damaged conditions [3, 4]. Therefore, a balanced regulation of survival and apoptosis is essential for controlling proper numbers of neural progenitors and postmitotic neurons, and in turn brain size.

Previously, the outbreak of Zika virus (ZIKV) in Brazil and its potential association with neurological disorders such as microcephaly and Guillain–Barré syndrome (GBS) have drawn global attention [5, 6]. Severe apoptosis and developmental defects have been detected in human neural progenitors, suggesting the link of ZIKV to microcephaly in humans [7–14]. Mouse models infected with ZIKV have confirmed

Haijun Zhang, Yafei Chang, Longbin Zhang and Seung-Nam Kim contributed equally to this work.

Electronic supplementary material The online version of this article (https://doi.org/10.1007/s12035-018-1358-4) contains supplementary material, which is available to authorized users.

✉ Tao Sun
taosun@hqu.edu.cn

[1] Department of Cell and Developmental Biology, Cornell University Weill Medical College, 1300 York Avenue, New York, NY 10065, USA

[2] School of Life Sciences and Technology, Shanghai Jiao Tong University, Shanghai 200240, China

[3] Center for Precision Medicine, School of Medicine and School of Biomedical Sciences, Huaqiao University, Xiamen 362021, China

[4] Department of Korean Medicine, Dongguk University, 32 Donggukro, Ilsandonggu, Goyangsi, Gyeonggido 10326, Republic of Korea

[5] State Key Laboratory of Molecular Developmental Biology, Institute of Genetics and Developmental Biology, Chinese Academy of Sciences, Beijing 100101, China

[6] Department of Virology, State Key Laboratory of Pathogen and Biosecurity, Beijing Institute of Microbiology and Epidemiology, Beijing 100071, China

the association of ZIKV and microcephaly [12, 15–18]. Screening drugs that inhibit ZIKV infection has been performed in 3-D-cultured organoids of human neural progenitors and human pluripotent stem cell-derived cortical neural progenitor cells [19, 20]. Moreover, molecular mechanisms that are associated with ZIKV infection and microcephaly are beginning to be revealed [21–25]. However, the mechanisms that regulate normal cell survival and apoptosis, and ZIKV-responding genes in the developing cortex are unclear.

Recent studies have shown that microRNAs (miRNAs) regulate development of the central nervous system (CNS) by controlling target gene expression [26, 27]. The RNase III member Dicer is responsible for miRNA biogenesis by cleaving precursor miRNA into mature miRNA [28]. Increased cell death has been detected in the mouse cortex by ablating Dicer expression [29, 30]. Knockdown or overexpression of miRNAs results in abnormal expression levels of their target genes that usually regulate survival and cell death, and causes cortical apoptosis [31]. However, which specific miRNAs play roles in regulating cell survival and cell death in the developing cortex remains unclear.

Here, we show that upregulation of miR-9 causes neuronal apoptosis, a great reduction of neural progenitors and newborn neurons, and results in smaller cortex. We find that expression level of miR-9 is increased, while GDNF, a putative target for miR-9, is downregulated after ZIKV infection in the cortex. Our results indicate that miR-9 and GDNF respond to ZIKV. Our studies further suggest an association of ZIKV infection, miR-9 upregulation, and microcephalic defects in mice.

Results

miR-9 Is Expressed in the Mouse Developing and Adult CNS

To determine functions of miR-9 in CNS development, we examined miR-9 expression patterns in the mouse CNS using in situ hybridization. DIG-labeled locked nucleic acid (LNA) probe for miR-9 was used. In a sagittal section of embryonic day 12.5 (E12.5) mouse whole embryo, miR-9 expression was mostly detected in the CNS, including the ventricular zone (VZ) in the cerebral cortex, midbrain, hindbrain, and the spinal cord, but not in the non-CNS tissues (Fig. 1a). Since E12.5 mouse cortices consist of neural stem cells (NSCs) and neural progenitors, high miR-9 cortical expression at this stage suggests its role in NSC and progenitor development. CNS-specific expression of miR-9 was maintained in the E15.5 embryo (Fig. 1b). In E15.5 brains, miR-9 was highly expressed in the cortical plate (CP) that contains newborn neurons, but not in neural progenitors resided in the VZ. In E18.5 brains, miR-9 displayed high expression in the CP, and its expression in the VZ and subventricular zone (SVZ) was low (Fig. S1A). In postnatal day 5 (P5) and 8-week-old adult brains, miR-9 had high expression levels in the olfactory bulb, cortex, and cerebellum but low expression in the subcortical region such as the striatum (Fig. 1c, d). Notably, miR-9 was expressed in hippocampus, with strong expression in the dentate gyrus (Fig. 1c, d). Our results indicate that miR-9 displays dynamic and region-specific expression in the developing and adult mouse CNS.

Cortical Upregulation of miR-9 Causes Microcephaly

Region-specific miR-9 expression in the CNS led us to speculate that miR-9 expression levels are critical for normal CNS development. To test this prediction, we generated a transgenic mouse model in which miR-9 expression is conditionally increased when the transgenic mouse is bred with a Cre line (Fig. 2a). Two loxP sites were cloned upstream of the miR-9-1 precursor, which is processed into mature miR-9 that displays the same sequence as processed from miR-9-2 and miR-9-3 precursors. In between the loxP sites, a Neo cassette and three poly-A repeats, which will generate a transcription stop signal, were cloned. In this transgenic line, called *miR-9-TG* in this study, miR-9 can be conditionally upregulated in any tissues and cells when crossed with tissue- or cell type-specific Cre mice (Fig. 2a).

To investigate the effect of increased miR-9 expression in cortical development, *miR-9-TG* mice were bred with a cortical-specific *Emx1-Cre* line [32], to generate conditional miR-9 overexpression mice, called *Emx1-miR-9* in this study. To test whether the transgene is expressed, we extracted RNA from the E12.5 cortices of *Emx1-miR-9* and control mice. Real-time reverse transcription PCR (RT-PCR) was performed using primers that are specific for the miR-9 transgene. The miR-9 expression level was significantly increased in the *Emx1-miR-9* cortex, indicating a successful Cre excision and an upregulation of miR-9 (Fig. 2b).

Strikingly, the cerebral cortex of *Emx1-miR-9* mice was significantly reduced compared to control litter mates at P1, while the other brain regions such as the cerebellum did not show obvious changes (Fig. 2c, d). Moreover, the wild-type and *miR-9-TG* mice without Cre did not show any detectable brain defects, thus, all were called the control group in this study. In E12.5 brains, while miR-9 upregulation did not alter the overall size of the cortex, the thickness of the cortical wall was greatly reduced in coronal brain sections with Nissl staining (Fig. 2e). The cortical wall of E15.5 *Emx1-miR-9* mice also was significantly reduced and the cortical plate was almost undetectable (Fig. 2f, h). In coronal sections of P1 *Emx1-miR-9* brains, a gap was detected between two hemispheres, the corpus callosum was not developed, and the cortical wall remained thinner than the control (Fig. 2g, h). These results show that increased miR-9 expression has a great impact on

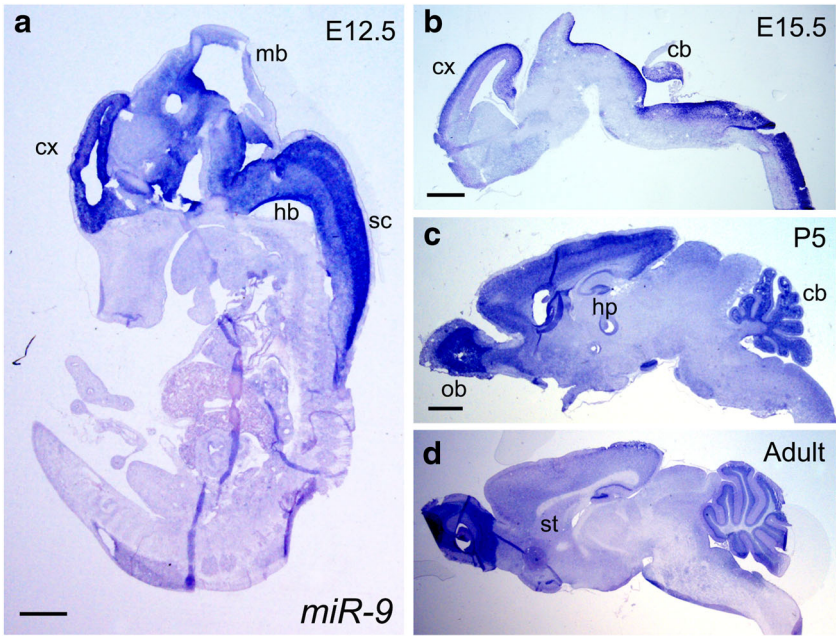

Fig. 1 miR-9 is expressed in the mouse developing and adult central nervous system. **a**, **b** In sagittal sections of mouse E12.5 and E15.5 embryos, miR-9 was expressed in the cerebral cortex (cx), midbrain (mb), cerebellum (cb), hindbrain (hb), and spinal cord (sc). In situ hybridization was performed using LNA probes for *miR-9*. **c** In the P5 brain, miR-9 expression was detected in the olfactory bulb (ob), cortex, hippocampus (hp), and cerebellum. **d** In an 8-week-old adult brain, high expression of miR-9 was observed in the olfactory bulb and cerebellum. miR-9 expression in the cortex, particularly in subcortical region such as the striatum (st), was decreased. Scale bar = 20 μm

early cortical development, notably resulting in a smaller cortex.

Increased miR-9 Expression Causes Neuronal Apoptosis

One mechanism of reduced cortical size is caused by increased apoptosis in neural progenitors and/or newborn neurons [33]. We thus analyzed whether the thinner cortical wall is associated with cell death due to miR-9 upregulation. In E12.5 *Emx1-miR-9* cortices, a significant apoptosis was detected in the VZ using a terminal deoxynucleotidyl transferase dUTP nick end labeling (TUNEL) assay (Fig. 3a, b). After DAPI nuclear staining, the number of healthy cells with round nuclei also was significantly reduced, suggesting a loss of normal cortical cells in E12.5 *Emx1-miR-9* cortices (Fig. 3c). Moreover, apoptosis was detected in E15.5 and P1 cortices, mostly in the cortical plate, not in the intermediate zone (IZ) and VZ/SVZ, suggesting more cell death in newborn neurons after E15.5 (Figs. S1B–E).

We next examined neural progenitor development. While BrdU labels cells in the S-phase, Ki67 labels cells in the G1-, S-, G2-, and M-phase. We found a great reduction in the percentages of $BrdU^+$ and $Ki67^+$ progenitors in E12.5 *Emx1-miR-9* cortex, compared to controls (Fig. 3d, g). Similarly, the percentages of Pax6- and Tbr2-expressing neural progenitors were significantly reduced in the *Emx1-miR-9* cortex (Fig. 3e–g). Our results indicate that upregulation of miR-9 results in a great reduction of proliferating cortical neural progenitors.

To further test whether apoptosis is specifically caused by miR-9, another CNS-enriched miRNA miR-124, which has been reported to promote neuronal differentiation [34], was ectopically expressed in the mouse embryonic cortex using in utero electroporation. Embryos were electroporated at E13.5 and brains were analyzed by anti-Caspase3 (Casp3) antibodies at E14.5. Similarly, miR-9 was electroporated in the E13.5 mouse cortex. While miR-9 ectopic expression caused increased apoptosis, which is consistent with the observation in *Emx1-miR-9* cortices, ectopic expression of miR-124 did not affect cell survival (Fig. S2). Our results suggest a specific effect of the miR-9 upregulation on neuronal cell death.

Upregulation of miR-9 Causes Decreased Cortical Neurogenesis

To test whether neurogenesis also is affected by increased miR-9 expression, we analyzed neuronal production in the cortex using markers for newborn neurons in the deep layer (Tbr1, Ctip2) and upper layer (Satb2) in E15.5 and P1 cortices. Numbers of cells positive for each marker and those stained with DAPI within a fixed column in the cortical wall were counted in control and *Emx1-miR-9* cortices. The percentages of numbers of these markers were significantly reduced in E15.5 and P1 *Emx1-miR-9* cortices, compared to those in controls, which were normalized to 100% for each marker (Fig. 4b, d, f; Fig. S3). Moreover, a percentage of the cell number for each marker versus that for DAPI was calculated and normalized to 100% for the control. The percentages of $Tbr1^+$ and $Satb2^+$ cells versus $DAPI^+$ cells were also reduced, indicating decreased cortical neurogenesis (Fig. 4b, d, f; Fig. S3). The percentage of Ctip2-expressing neurons did

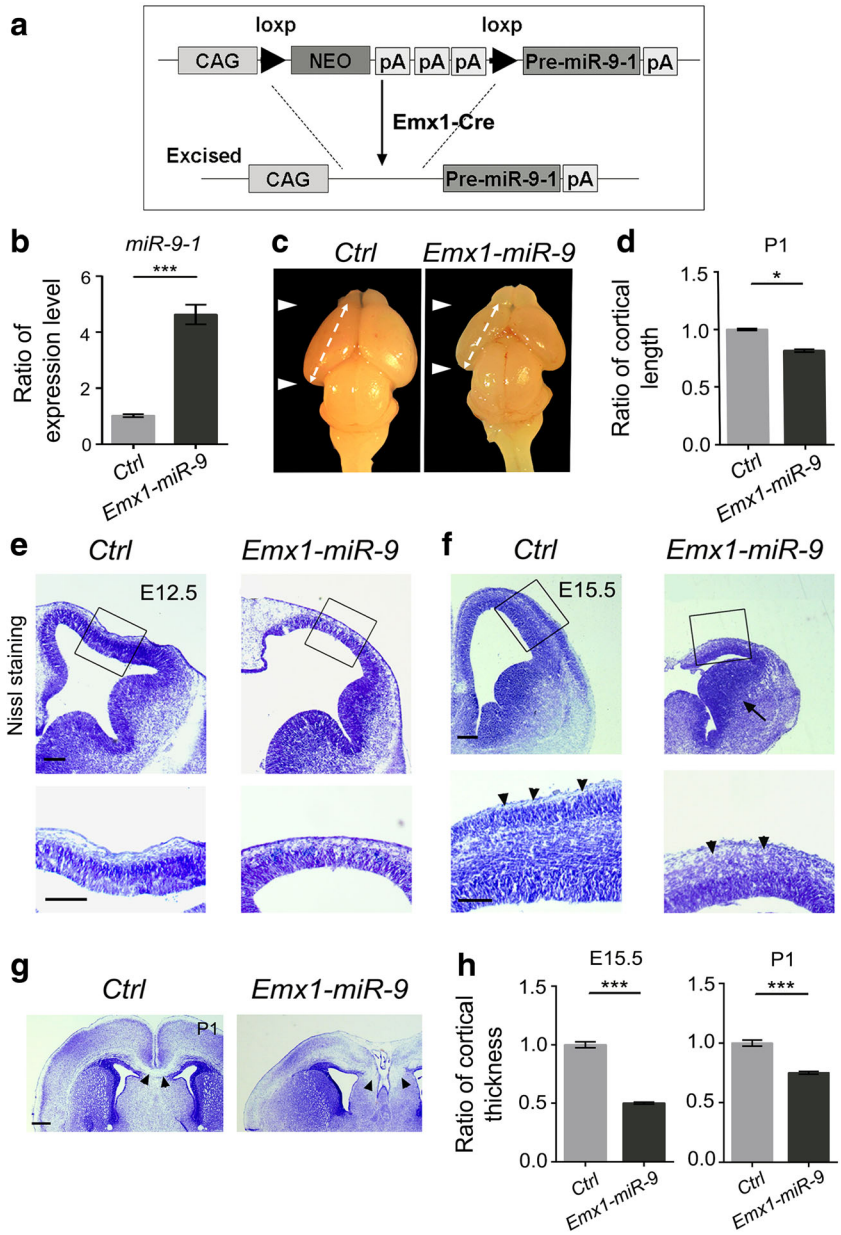

Fig. 2 Cortical specific upregulation of miR-9 results in a smaller cortex. **a** The transgene of *miR-9-1* precursor was driven by the *CAG* promoter followed by a floxed poly-A stop cassette. Conditional activation by breeding with the cortical-specific *Emx1-Cre* mouse line permitted overexpression of miR-9 in the cortex. **a** miR-9 upregulation was detected in *Emx1-miR-9* transgenic cortices, with higher expression levels than the wild type control (*Ctrl*), as detected by real-time reverse transcription PCR. Values represent mean ± SEM. $n = 3$ different brains, $^{***}P < 0.001$. Student's *t* test was used. **c** The cortex of P1 *Emx1-miR-9* mice was greatly reduced. The arrowheads show the most rostral and caudal regions in the cortex. The dashed lines show measurement of the cortical length. **d** The cortical length was greatly reduced in P1 *Emx1-miR-9* mouse brains than those in controls. **e** The cortical wall was thinner than controls in E12.5 *Emx1-miR-9* mice, detected by Nissl staining. **f** The cortex of *Emx1-miR-9* mice was smaller and the cortical wall was thinner than controls at E15.5. While the cortical plate (arrowheads) was undetectable in *Emx1-miR-9* mice, the subcortical region (arrow) appeared normal. The squared regions are shown in high-power views. **g** The cortex of P1 *Emx1-miR-9* mice was greatly reduced. The corpus callosum (arrowheads) was not developed, compared to controls. The cortical wall was thinner than controls, detected by Nissl staining. **h** Quantification of the thickness of the E15.5 and P1 cortical wall, the thickness of the control cortical wall was normalized to 1. Values represent mean ± SEM. $n = 3$ different brains, each brain had two sections. $^{***}P < 0.001$. Student's *t* test was used. Scale bar = 20 μm

not display significant reduction, suggesting a selective alteration of neuronal population by increased miR-9 expression. Our results indicate that miR-9 upregulation causes decreased neurogenesis.

Gdnf Is a Target for miR-9

miRNAs normally function through silencing target mRNAs. To analyze the mechanism of miR-9 regulation on apoptosis,

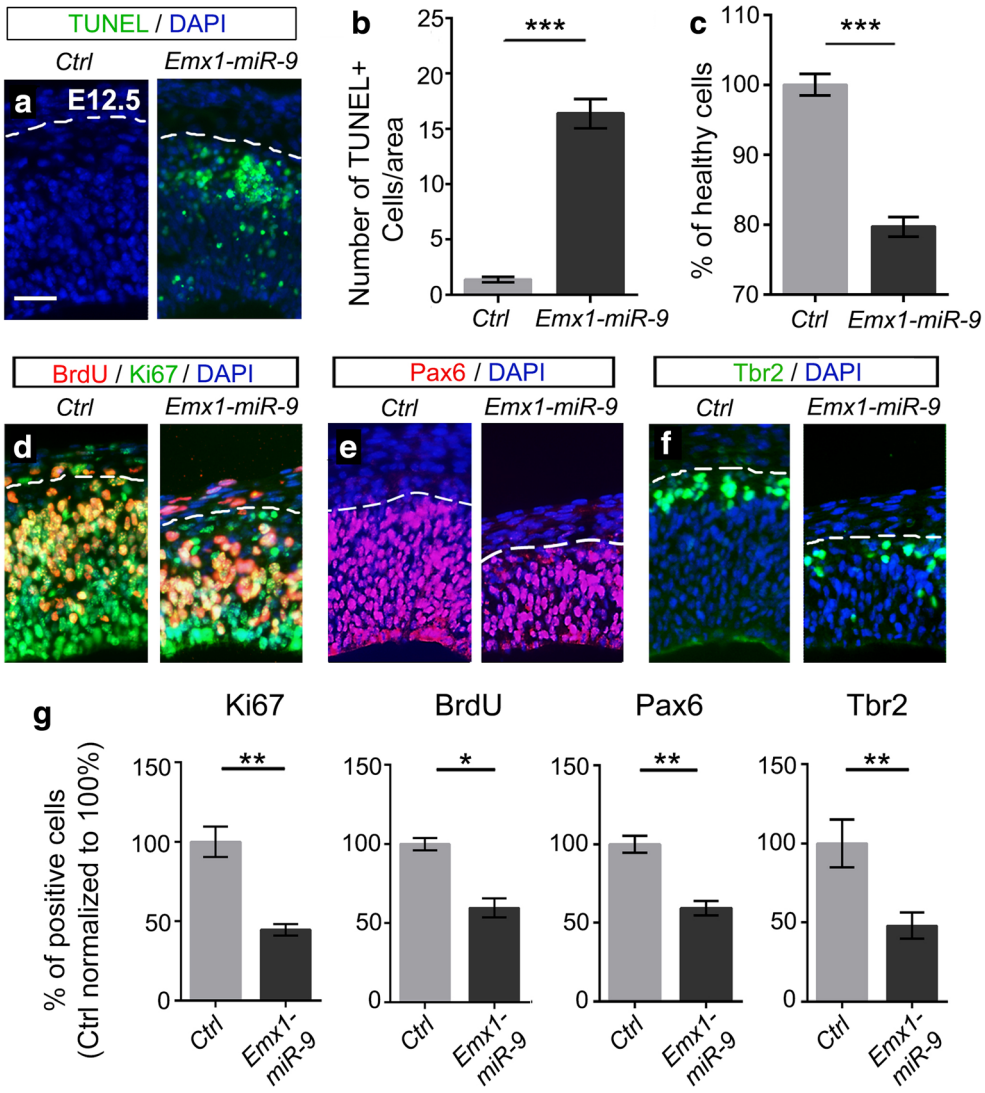

Fig. 3 Cortical upregulation of miR-9 causes apoptosis and reduced neural progenitors. **a**, **b** Increased apoptosis was observed in E12.5 *Emx1-miR-9* cortices compared to controls (*Ctrl*), as detected by TUNEL assays (**a**) and the number of TUNEL$^+$ cells in a fixed area in the section under the microscope (**b**). **c** Quantification of cells with round nuclei after DAPI staining, shown as percentage compared to all DAPI$^+$ cells in a fixed area in the section under the microscope. **d**–**f** The numbers of BrdU$^+$, Ki67$^+$, Pax6$^+$, and Tbr2$^+$ neural progenitors were greatly reduced in E12.5 *Emx1-miR-9* cortices, compared to controls. **g** The percentages of the numbers of BrdU$^+$, Ki67$^+$, Pax6$^+$, and Tbr2$^+$ neural progenitors versus those of DAPI$^+$ cells in a fixed area in the section under the microscope were greatly reduced in E12.5 *Emx1-miR-9* cortices. Values represent mean ± SEM. $n = 3$ different brains, each brain had at least three sections. $^*P < 0.05$; $^{**}P < 0.01$; $^{***}P < 0.001$. Student's *t* test was used. Scale bar = 50 μm

we examined predicted targets that are related to cell survival. By searching a well-established miRNA target prediction tool TargetScan database (www.targetscan.org), we found that the 3′UTR in glial cell-derived neurotrophic factor (*Gdnf*) contains a miR-9 targeting site (Fig. 5a). To test whether *Gdnf* is a target, the 3′UTR of *Gdnf* was cloned into a *luciferase* vector. miR-9 but not miR-9 mutation had a significant silencing effect on *Gdnf* 3′UTR, as demonstrated by reduced luciferase activity (Fig. 5b). Furthermore, the luciferase activity of the construct containing mutations in the miR-9 targeting site within the *Gdnf* 3′UTR was not affected by miR-9 co-expression, indicating that *Gdnf* is a specific target for miR-9 (Fig. 5b).

GDNF Protects Neuronal Apoptosis Induced by miR-9

Previous studies have shown that GDNF protects neurons from apoptosis [3, 4]. To test whether GDNF is a survival factor for neural progenitors in the developing cortex, we used short hairpin RNA (shRNA) for *Gdnf* (*shGdnf*) to knock down its expression level. The control pCAGIG construct and the scramble shRNA were used to examine the knockdown effect of *shGdnf*. Neither the control construct nor the scramble shRNA showed activity (Fig. S4). *ShGdnf* was electroporated into E13.5 cortices and analyzed at E14.5. While the control pCAGIG construct did not cause apoptosis, *shGdnf* induced severe cell death, as demonstrated by Casp3 immunohistochemistry, indicating a positive role of GDNF in cell survival in the developing cortex (Fig. 5c–e).

If *Gdnf* is a functional target of miR-9, ectopic expression of the 3′UTR of *Gdnf* should make miR-9 bind to its 3′UTR and reduce miR-9 silencing activity. As a result, apoptosis induced by increased miR-9 expression should be rescued by the *Gdnf* 3′UTR. We thus cloned the *Gdnf* 3′UTR and co-electroporated it together with miR-9 in E13.5 cortices and analyzed at E14.5. The *Gdnf* 3′UTR significantly rescued apoptosis defects caused by increased miR-9 expression (Fig. 5f, g, i). However, mutations of the miR-9 targeting site within

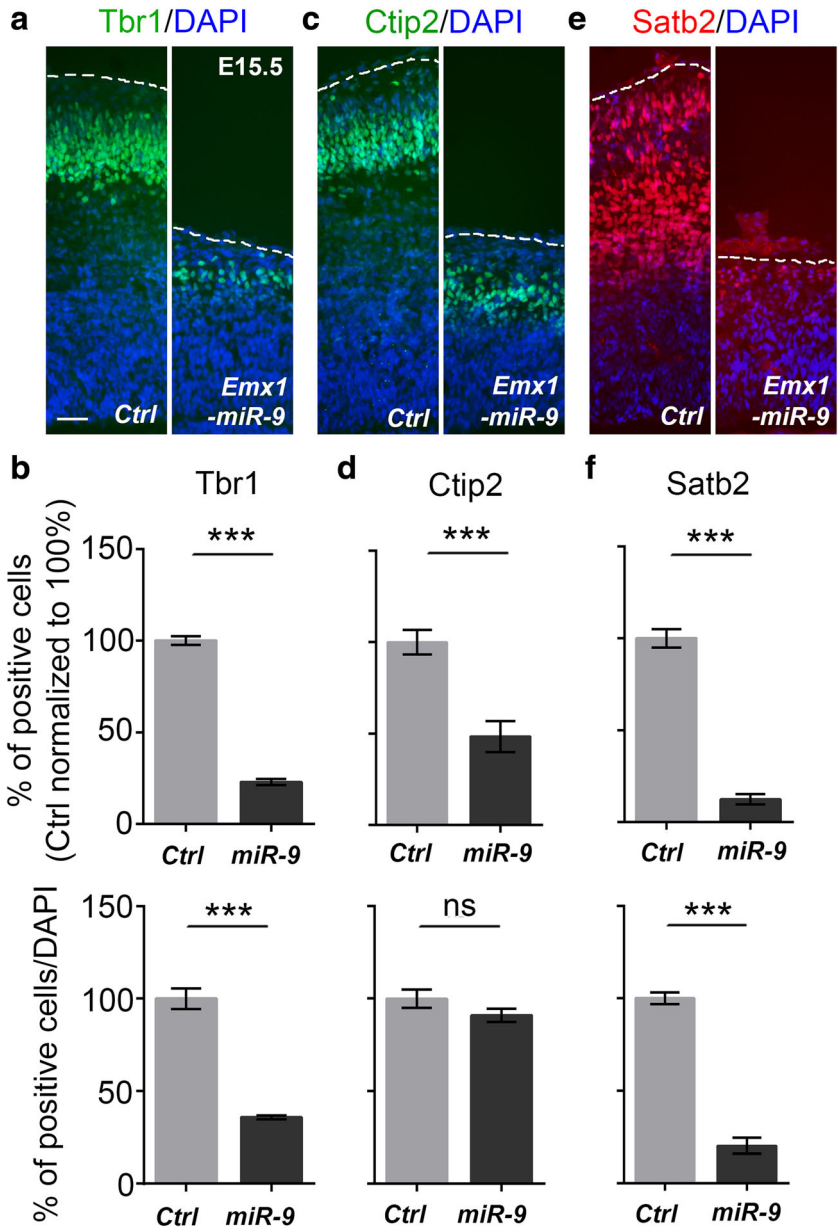

Fig. 4 Cortical upregulation of miR-9 causes decreased neuronal production at E15.5. **a**, **b** miR-9 upregulation in E15.5 *Emx1-miR-9* cortices caused a reduction in the percentage of the number of Tbr1-expressing neurons and the percentage of Tbr1-expressing neurons versus DAPI positive cells, compared to those controls (*Ctrl*) that was normalized to 100%. **c**, **d** The percentage of the number of Ctip2-expressing neurons but not the percentage of Ctip2-expressing neurons versus DAPI positive cells was reduced in *Emx1-miR-9* cortices. **e**, **f** miR-9 upregulation in E15.5 *Emx1-miR-9* cortices caused a reduction in Satb2-expressing neurons. Values represent mean ± SEM. $n = 3$ different brains, each brain had at least three sections. $^{***}P < 0.001$; *ns* not significant. Student's *t* test was used. Scale bar = 100 μm

the *Gdnf* 3′UTR failed to rescue apoptosis defects caused by increased miR-9 expression (Fig. 5f, h, i). These results suggest that GDNF plays a protective role in neuronal survival by serving as a specific target for miR-9.

ZIKV Causes Reduction of Neural Progenitors and Newborn Neurons

The microcephalic defects in miR-9 overexpression mice resembled those of ZIKV-infected mice. We speculated that miR-9 expression might be associated with ZIKV infection. We first examined development of neural progenitors and newborn neurons in ZIKV-infected mouse embryonic cortex. ZIKV SZ01 was injected in one side of the ventricle in E13.5 mouse cortex. Brains were analyzed at E18.5, 5 days after infection (Fig. 6). In the injected side, the cortical wall and the ventral cortical region were severely infected by ZIKV, as detected by a ZIKV antibody made from a convalescent patient serum, suggesting that ZIKV can effectively replicate in the mouse embryonic cortex (Fig. 6a, b).

In the cortex, while Sox2 is mostly expressed in radial glial cells (RGCs), Tbr2 is expressed in intermediate progenitors (IPs) [35, 36]. We quantified numbers of neural progenitors and found that the percentages of Sox2- and Tbr2-expressing progenitors are significantly reduced in the ZIKV-infected side, compared to the opposite side, in the E18.5 cortex (Fig. 6c–f). Moreover, we examined the expression of markers of newborn neurons such as Tbr1 and Satb2 [36]. The

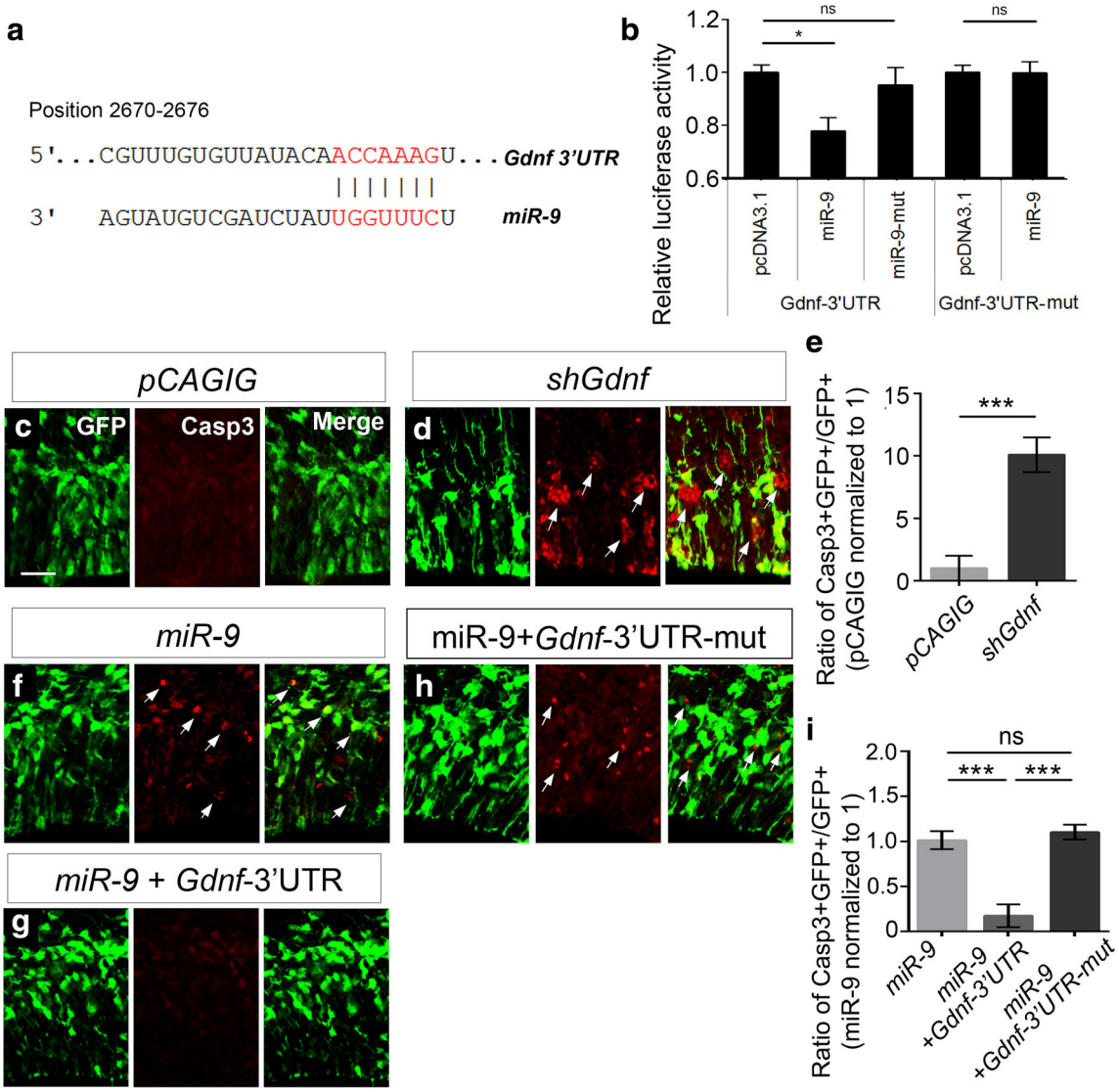

Fig. 5 *Gdnf* is a putative target for miR-9 and protects neuronal apoptosis caused by miR-9 upregulation. **a** The 3′UTR of *Gdnf* contained one miR-9 binding site. **b** Activity of *luciferase* containing the 3′UTR of *Gdnf* was reduced when co-expressed with miR-9. miR-9 had no silencing effects in the *Gdnf* 3′UTR containing mutations in the miR-9 binding site. $n = 3$. $^*P < 0.05$; *ns* not significant. Student's *t* test was used. **c**–**e** While the pCAGIG vector had no effects on causing cell death, knocking down GDNF expression using *shGdnf* using in utero electroporation in wild-type mouse cortices resulted in apoptosis, as detected by Casp3-expressing cells (arrows). **f**–**i** Ectopic expression of the 3′UTR of *Gdnf* (*Gdnf-3′UTR*) that contains the miR-9 binding site was able to block miR-9 effect of inducing apoptosis. However, mutations of miR-9 binding sites in the *Gdnf-3′UTR* failed to rescue apoptosis caused by miR-9 expression. Values represent mean ± SEM. $n = 3$ different brains, each brain had at least three sections. $^{***}P < 0.001$; *ns* not significant. Student's *t* test was used. Scale bar = 50 μm

percentages of Tbr1- and Satb2-expresssing neurons were greatly reduced, compared to the uninjected control side (Fig. 6g–j). These results indicate that ZIKV infection reduces the neural progenitor population and decreases neurogenesis, which may lead to microcephaly.

miR-9 and Its Target GDNF Respond to ZIKV

Reduced neural progenitors and neurons after ZIKV infection suggest that genes regulating neurogenesis might be affected by ZIKV. Because miR-9 upregulation also caused microcephaly, we tested whether miR-9 responds to ZIKV. ZIKV was injected into the ventricle of E13.5 mouse embryonic cortex, and brain tissues were analyzed at E16.5. miR-9 consists of three isoforms: miR-9-1, miR-9-2, and miR-9-3 with highly conserved seed sequence in mice (Fig. 7a). Depending on directions of miRNA biogenesis, mature miR-9 is processed as miR-9-5p and miR-9-3p. Thus, expression levels of miR-9-5p and miR-9-3p were quantified by real-time RT-PCR (Fig. 7b). Compared to that of control brains injected with culture medium, expression of both miR-9-5p and miR-9-3p was upregulated upon ZIKV injection (Fig. 7b). These results suggest that miR-9 responds to ZIKV infection in the developing cortex.

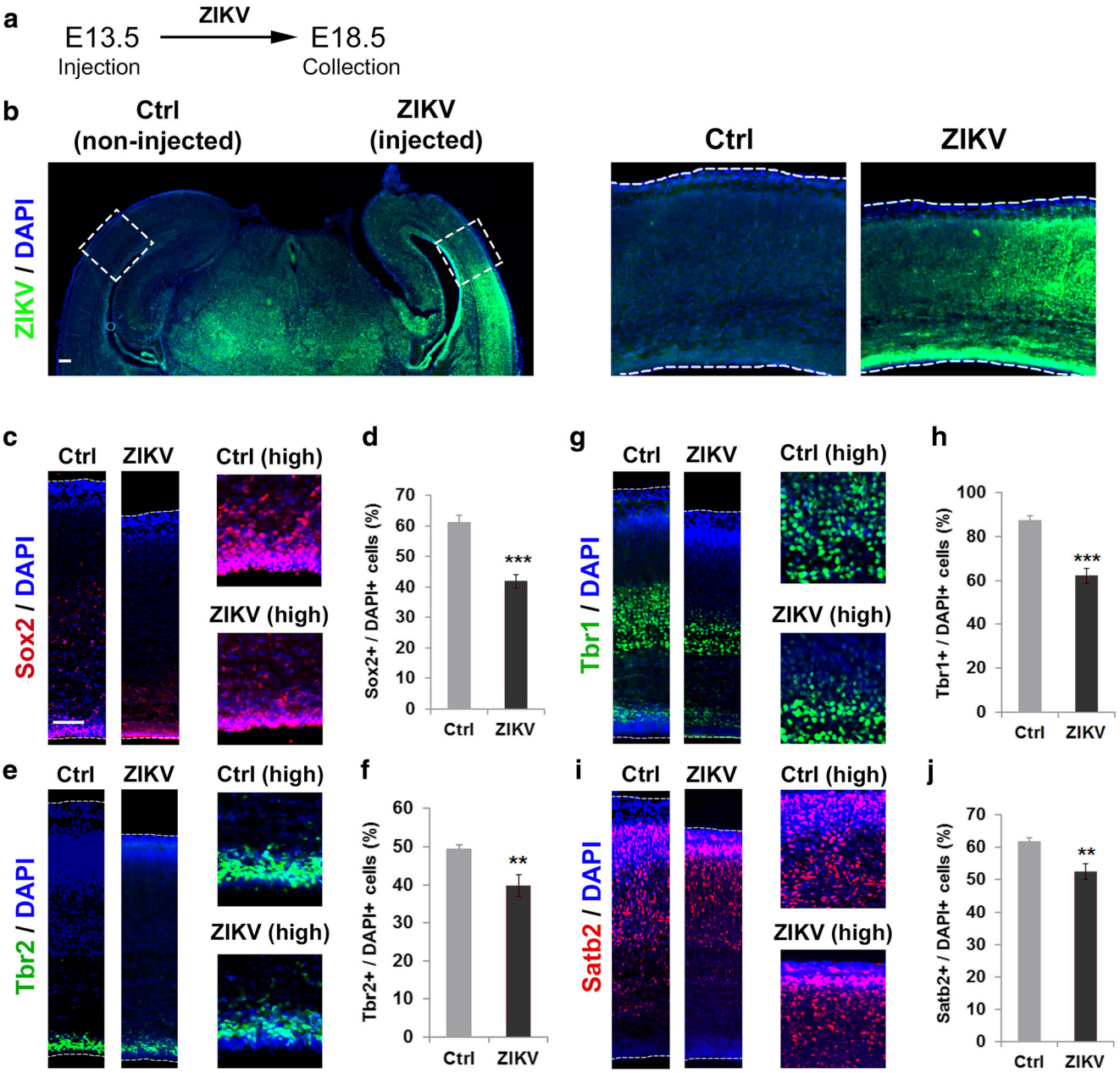

Fig. 6 ZIKV causes reduction of neural progenitors and newborn neurons. **a**, **b** Infection of ZIKV in the embryonic cortex, injected at E13.5 and analyzed at E18.5. **c**–**f** The percentages of Sox2- and Tbr2-expressing progenitors were significantly reduced in the ZIKV-infected side, compared to the opposite side, in the E18.5 cortex. **g**–**j** The percentages of Tbr1- and Satb2-expresssing neurons were greatly reduced, compared to the uninjected control side. Values represent mean ± SEM. $n = 3$ different brains, each brain had two sections. $^{***}P < 0.001$. Student's t test was used. Scale bar = 50 μm

Because ZIKV caused an increased expression of miR-9, if *Gdnf* is a target for miR-9, expression level of GDNF should be downregulated after ZIKV infection. We thus examined GDNF expression in E16.5 cortices that was infected with ZIKV at E13.5. GDNF expression was mostly detected in the intermediate zone and deep layers of the cortical plate in E16.5 control cortex (Fig. 7c). In the cortex infected with ZIKV, the expression pattern of GDNF was not changed, the expression level of GDNF in the IZ and CP was decreased, compared to the control cortex (Fig. 7c, d). Moreover, *Gdnf* mRNA level also was reduced in ZIKV-infected cortex, as detected by real-time RT-PCR (Fig. 7e). These results suggest that miR-9 target gene *Gdnf* also responds to ZIKV.

Furthermore, to test whether other known miR-9 target genes also were affected by miR-9 upregulation due to ZIKV infection, we examined expression levels of *Bcl2l11*, *Rest*, *Hes1*, *Hdac5*, and *Foxp2* using real-time RT-PCR. Except *Hdac5*, expression levels of *Bcl2l11*, *Rest*, *Hes1*, and

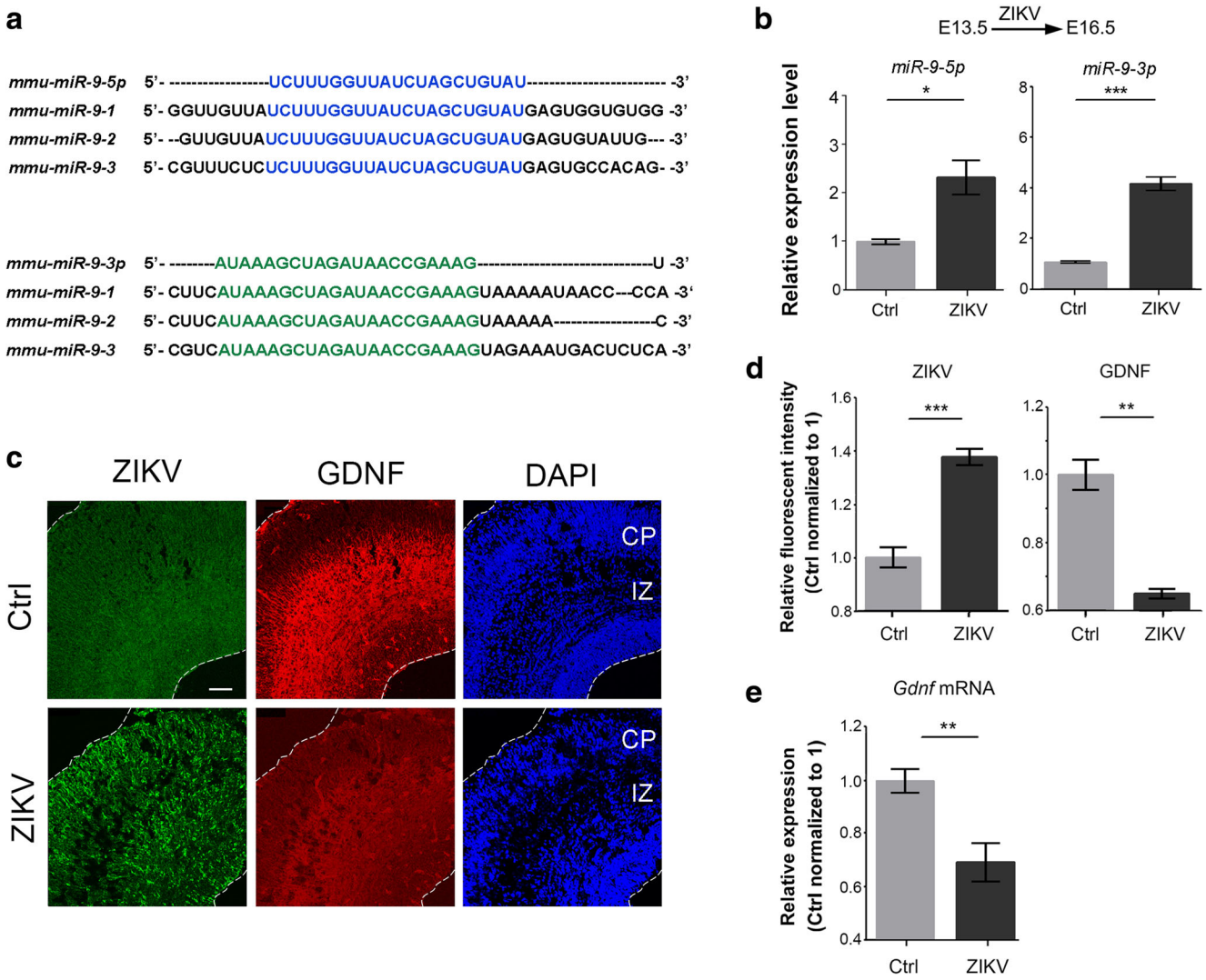

Fig. 7 miR-9 and its target gene GDNF respond to ZIKV. **a** Biogenesis of mature miR-9 is processed as miR-9-5p and miR-9-3p. **b** Expression levels of mature miR-9-5p and miR-9-3p were upregulated after ZIKV injection. The mouse embryonic cortex was injected with ZIKV at E13.5 and analyzed at E16.5. **c**, **d** GDNF expression was mostly detected in the intermediate zone (IZ) and deep layers of the cortical plate (CP) in E16.5 control (Ctrl) cortex. In the cortex infected with ZIKV, the expression pattern of GDNF was not changed, the expression level of GDNF in the IZ and CP was decreased, compared to the control cortex, detected by immunohistochemistry. **e** *Gdnf* mRNA level was reduced in ZIKV infected cortex, as detected by real-time RT-PCR. Values represent mean ± SEM. $n = 3$ different brains, each brain had two sections. $^{**}P < 0.01$; $^{***}P < 0.001$; Student's t test was used

Foxp2 were decreased (Fig. S5A–E). On the other hand, expression levels of *Vegfa* and *Mecp2*, which are not predicted targets for miR-9, displayed increased expression (Fig. S5G, H). Consistent with immunohistochemistry on brain sections, expression of *Sox2* mRNA also was decreased (Fig. S5F). These results suggest that upregulation of miR-9 in ZIKV-infected brains causes increased expression of miR-9 target genes, and might in turn affect neural progenitor development.

Discussion

Accumulating evidence has shown that miRNAs play crucial roles in many aspects of neural development, such as proliferation of neural progenitors, neuronal survival, and cell fate choices for neurons and glia [37–39]. We here show that transgenic mice with miR-9 overexpression in the developing cortex display a smaller cortex, and ZIKV infection induces the upregulation of miR-9. We further demonstrate that GDNF is a specific target for miR-9, and ectopic expression of the 3′ UTR of *Gdnf* but not its mutation is sufficient to block miR-9-induced apoptosis in vivo. Our results suggest a protective role of GDNF from cell death by damping miR-9 apoptotic effect.

miR-9 is involved in various processes of CNS development in different organisms. In zebrafish, miR-9 was shown to control the formation of the midbrain–hindbrain boundary (MHB) and the timing of neurogenesis [40, 41]. In *Xenopus*,

miR-9 knockdown causes apoptosis in the forebrain [42]. In chick embryos, miR-9 controls specification of distinct motor neuron subtypes in the developing spinal cord [43, 44]. In the mouse brain, miR-9 specifically targets prelamin A but not lamin C [45]. miR-9 is highly expressed in the cortical hem and promotes generation of Cajal-Retzius neurons [46]. miR-9 function is required for regulating cortical size, since miR-9 ablation results in a smaller cortex [47]. miR-9 also functions in radial migration of cortical projection neurons [48]. In summary, miR-9 plays distinct roles in proliferation, survival, and migration of neural progenitors and mature neurons in a specific cell-context manner [49, 50]. Therefore, the level of miR-9 expression appears to be critical to normal neurogenesis in the CNS. Here, we have uncovered an unexpected role of miR-9 dosage regulation—neuronal apoptosis caused by miR-9 upregulation.

In the developing cortex, apoptosis is a precisely controlled event that ensures proper numbers of neural progenitors and mature neurons, and in turn, the cortical size [33]. A major defect in brains of *Dicer* conditional knockout mice, in which miRNA biogenesis is blocked in the CNS or specifically in the cortex, is apoptosis, indicating a critical role of miRNAs in neuronal survival [30, 31]. Our studies here have shown that increased miR-9, similar to miR-9 knockdown, causes neuronal apoptosis, suggesting that proper miR-9 expression level is crucial for cell survival. We cannot rule out the side effect of overexpressing miR-9 in the cortex, which might also result in cell death due to mis-targeting other genes by miR-9 upregulation. Nevertheless, we have found that overexpression of another brain-enriched miRNA miR-124 has no effect on cell survival, the apoptotic effect is likely to be miR-9 specific.

The recent emergence of Zika virus in the Americas has coincided with increased reports of babies born with microcephaly. ZIKV has been detected in the placenta and amniotic fluid of two women with microcephalic fetuses [51, 52], and in the brain tissue of aborted microcephalic fetus and retinas of microcephalic infants [53, 54]. Furthermore, mouse models infected with ZIKV have been shown to display microcephaly, mostly caused by apoptosis defect and reduced neural progenitors [12, 15, 16]. However, downstream target genes affected by ZIKV infection are not clear [24, 25, 55]. Our study has shown an association between increased miR-9 expression after ZIKV infection, and apoptosis in neural progenitors and newborn neurons caused by miR-9 upregulation. Our data suggest that miR-9 is likely one of the downstream genes that mediate cortical defects caused by ZIKV infection, which eventually leads to microcephaly.

Furthermore, we have found that the neurotrophic factor GDNF is a putative target of miR-9, and GDNF responds to ZIKV and is downregulated by ZIKV infection in the embryonic cortex. Previous studies have demonstrated neuroprotective roles of GDNF in neural injuries, particularly spinal cord injuries [56–58]. While miR-9 function is required for proper proliferation and differentiation of cortical neurons, one side effect of increased miR-9 expression is perhaps to induce apoptosis. The maintenance of GDNF expression in the developing cortex might be to protect neurons from miR-9-induced apoptosis by serving as its target gene. Moreover, because one miRNA can have many target genes, our studies here only demonstrate one major target for miR-9 in apoptotic effects. More targets for miR-9 in specific cells and in a specific functional event are required to be established in the future, in particular in ZIKV-infected brains.

Overall, our results suggest an association of ZIKV-mediated upregulation of miR-9 expression and apoptosis in the mouse cortex, which partly accounts for smaller cortex. Moreover, ZIKV infection is also associated with other neurological disorders [5, 6]. It would be interesting to investigate downstream genes of ZIKV in these disorders in the future.

Experimental Procedures

Generating miR-9 Conditional Overexpression Mice

Transgenic mice were generated using the construct, called here pCBR, which is based on the pBigT vector as a backbone. Three poly-A repeats that generate a transcription stop signal was cloned at the 3′-end of a Neo cassette. The Neo-poly-A DNA fragment was flanked by two loxP sites. The precursor sequence of the mouse miR-9-1 was further cloned at the 3′-end of the second loxP site. The loxP-Neo-poly-A-loxP-miR-9-1 DNA fragment was subcloned at the 3′-end of the cytomegalovirus (CMV) early enhancer element and chicken beta-actin (*CAG*) promoter. The insert was purified and injected into fertilized eggs to generate conditional *miR-9* overexpression transgenic mice (*miR-9-TG*) at the Core facility of Weill Cornell Medical College. Three transgenic founder lines were analyzed and only one line was focused in this study. Moreover, the wild-type and *miR-9-TG* mice without Cre did not show any detectable brain defects, thus, all were called the control group in this study.

The *miR-9* transgenic line was bred with the *Emx1-Cre* line to conditionally overexpress miR-9 only in the cerebral cortex due to the *Emx1* enhancer activity [32]. Positive mice were genotyped using primers for both *Cre* and *Neo*: Cre-F: 5′-TAAAGATATCTCACGTACTGACGGTG-3′ and Cre-R 5′-TCTCTGACCAGAGTCATCCTTAGC-3′; Neo-F: 5′-CAGATCATCCTGATCGACAAG-3′ and Neo-R: 5′-GACCTGCAGCCAATATGGGATC-3′.

For staging of embryos, midday of the day of vaginal-plug formation was considered as E0.5; the first 24 h after birth were defined as P0. Animal use was overseen by the Animal Facility at Weill Cornell Medical College, and was performed according to the institutional ethical guidelines for animal experiments.

Zika Virus Preparation and Animal Infection

The Asian lineage ZIKV strain SZ01 (GenBank accession number: GEO KU866423) and the ICR mouse line were used in this study. One microliter of Zika virus stock (6.5×105 PFU/ml) was injected into one side of the lateral ventricle of ICR mouse brains at E13.5 through in utero injection, culture medium (RPMI medium 1640 basic + 2% FBS) was injected as mock controls. The injected brains were collected at E16.5 and E18.5. Total RNA was extracted from the dorsal cortical region. At least three experimental pregnant animals and three control pregnant animals were injected with virus and PBS, respectively, in order to collect embryonic brains at each developmental stage. At least three infected brains from three different pregnant mice were used for either real-time qRT-PCR or immunohistochemistry. All experimental procedures were performed according to protocols approved by the Institutional Animal Care and Use Committee at Beijing Institute of Microbiology and Epidemiology.

BrdU Pulse to Analyze Proliferation

To analyze proliferation of neural progenitor cells in developing cortex, one dose of BrdU (50 mg/g body weight) was administrated by intraperitoneal (I.P.) injection to mice at 1 h before sacrifice.

Tissue Preparation and Immunohistochemistry

Mouse brains were fixed in 4% paraformaldehyde (PFA) in phosphate-buffered saline (PBS) over night, incubated in 25–30% sucrose in PBS, embedded in OCT, and stored at − 80 °C until use. Brains were sectioned (14–16 μm) using a cryostat. For antigen recovery, sections were incubated in heated (95–100 °C) antigen recovery solution (1 mM EDTA, 5 mM Tris, pH 8.0) for 15–20 min, and cooled down for 20–30 min. Before applying antibodies, sections were blocked in 10% normal goat serum (NGS) in PBS with 0.1% Tween-20 (PBT) for 1 h. Sections were incubated with primary antibodies at 4 °C overnight and visualized using goat anti-rabbit IgG–Alexa-Fluor-488 and/or goat anti-mouse IgG–Alexa-Fluor-546 (1:300, Molecular Probes) for 1.5 h at room temperature. Images were captured using a Leica digital camera under a fluorescent microscope (Leica DMI6000B) or a Zeiss confocal microscope.

Primary antibodies against the following antigens were used: bromodeoxyuridine (BrdU) (1:50, Developmental Studies Hybridoma Bank at University of Iowa (DSHB)), Ki67 (1:500, Abcam), Pax6 (1:500, Covance), Pax6 (1:15, DSHB), Tbr1 (1:500, Abcam), Tbr2 (1:500, Abcam), activated Caspase 3 (1:1000, R&D), Ctip2 (1:1000, Abcam), Satb2 (1:500, Abcam), GFP (1:1000, Abcam, chicken), GFP (1:1000, Rockland, rabbit), and Activated-caspase3 Casp3 (CST, 9664s, 1:500). Nuclei were stained with DAPI (Invitrogen, 1:1000).

Cell Counting in Brain Sections

Cell counting in the mouse brain sections was performed on a fixed width (200 μm bin) of a representative column in the cortical wall. All sections analyzed were selected from a similar medial point on the anterior-posterior axis. Cell counting was performed in minimal three chosen areas in each brain, and at least three brains were analyzed in each group. Cell counting in each chosen area was repeated manually at least three times and a mean was obtained.

Moreover, the positive cells for each marker were normalized to 100% in the control cortex and were then compared with those in the *Emx1-miR-9* cortex. Next, the percentage was calculated by dividing the positive cell numbers for each marker with the numbers of DAPI positive cells for either the control or the *Emx1-miR-9* cortex. To facilitate the comparison, the percentage of the control cortex was then set as 100%.

For ZIKV-infected brains, ZIKV-infected areas were randomly chosen, the mirrored areas of un-infected side in the cortex were selected accordingly. A fixed width (200 μm bin) of the selected area in the cortical wall was used for cell counting. Cell counting was performed manually in each brain section, and at least three sections from each brain and at least three brains were analyzed. Cell counting in each chosen area was repeated manually at least three times and a mean was obtained.

ZIKV Detection

To detect ZIKV expression, the primary ZIKV antibody (1:100) was made from a convalescent patient serum [59]. Goat anti-human FITC was used as the second antibody.

Terminal Deoxynucleotidyl Transferase-Mediated dUTP Nick End Labeling Assay

The terminal deoxynucleotidyl transferase dUTP nick end labeling (TUNEL) assay was described previously [60]. Briefly, to identify apoptotic cells in the cortex, a TUNEL assay was performed using an Apop Tag Fluorescein in situ Apoptosis detection kit (Chemicon) on 14-μm frozen sections according to the manufacturer's protocols.

In Utero Electroporation

In utero electroporation was performed in E13.5 embryos according to the published protocol [61]. Briefly, plasmid DNA was prepared using the EndoFree Plasmid Maxi Kit (QIAGEN) according to manufacturer's instructions, and diluted to 2 μg/μl. DNA solution was injected into the lateral

ventricle of the cerebral cortex, and electroporated with five 50-ms pulses at 35 V using an ECM830 electrosquareporator (BTX). Embryos were allowed to develop to E14.5. Animals with the brains electroporated, as detected by the GFP fluorescence under a fluorescent dissection scope (Leica, MZ16F), were selected for further analyses. Cell counting was performed in minimal three chosen areas in each brain, and at least three electroporated brains for each construct were analyzed. Cell counting in each chosen area was repeated at least three times and a mean was obtained.

In Situ Hybridization

In situ hybridization for miRNA expression was performed on frozen sections using locked nucleic acid (LNA) probes. Such probes contain modified nucleotides that form a locked structure to stabilize LNA/RNA duplex, thus have been widely used to detect miRNA expression. After fixation with 4% paraformaldehyde (PFA), acetylation with acetylation buffer (1.3% Triethanolamine, 0.25% Acetic anhydride, 20 mM HCl), treatment with proteinase K (5 μg/ml, IBI Scientific), and pre-hybridization (1 × SSC, 50% Formamide, 0.1 mg/ml Salmon Sperm DNA Solution, 1 × Denhart, 5 mM EDTA, pH 7.5), brain sections were hybridized with DIG-labeled LNA probes at Tm-22 °C overnight. After washing with pre-cooled wash buffer (1 × SSC, 50% Formamide, 0.1% Tween-20) and 1 × MABT, sections were blocked with blocking buffer (1× MABT, 2% Blocking solution, 20% heat-inactivated sheep serum) and incubated with anti-DIG antibody (1:1500, Roche) at 4 °C overnight. Brain sections were washed with 1× MABT and Staining buffer (0.1 M NaCl, 50 mM $MgCl_2$, 0.1 M Tris-HCl, pH 9.5), stained with BM purple (Roche) at room temperature until ideal intensity was reached. The miR-9 LNA probes (Exiqon) were 3′- and 5′-end labeled with DIG–ddUTP.

Statistics

All experiments were repeated at least with three biological replicates. All results are presented as mean ± standard error of the mean (S.E.M.). *P* values were determined by unpaired Student's *T* test for assessing the significance of differences between two groups. *P* values < 0.05 were considered significant. Significant differences were denoted as "*" *P* values < 0.05, "**" *P* values < 0.01, "***" *P* values < 0.001.

Acknowledgements We thank members of the Sun laboratory for their valuable discussions and advice. This work was supported by an award from the Hirschl/Weill-Caulier Trust (T. S.), an R01-MH083680 grant from the NIH/NIMH (T. S.) and the National Natural Science Foundation of China (81471152, 31771141 and 81701132).

Author Contributions G.O., Z.X., and T.S. designed the experiments. H.Z., Y.C., L.Z., S.K., G.O., Z.Z., T.M., and C.L. performed the experiments. H.Z., Y.C., L.Z., G.O., Z.Z, Y.N., C.Q., and T.S. analyzed and interpreted the data. T.S. wrote the manuscript and supervised the project.

Compliance with Ethical Standards

Conflict of Interest The authors declare that they have no conflict of interest.

References

1. Woods CG, Parker A (2013) Investigating microcephaly. Arch Dis Child 98:707–713. https://doi.org/10.1136/archdischild-2012-302882
2. Depaepe V, Suarez-Gonzalez N, Dufour A, Passante L, Gorski JA, Jones KR, Ledent C, Vanderhaeghen P (2005) Ephrin signalling controls brain size by regulating apoptosis of neural progenitors. Nature 435:1244–1250
3. Wang Y, Chang CF, Morales M, Chiang YH, Hoffer J (2002) Protective effects of glial cell line-derived neurotrophic factor in ischemic brain injury. Ann N Y Acad Sci 962:423–437
4. Burke RE (2006) GDNF as a candidate striatal target-derived neurotrophic factor for the development of substantia nigra dopamine neurons. J Neural Transm Suppl:41–45
5. Ladhani SN, O'Connor C, Kirkbride H, Brooks T, Morgan D (2016) Outbreak of Zika virus disease in the Americas and the association with microcephaly, congenital malformations and Guillain-Barre syndrome. Arch Dis Child 101:600–602. https://doi.org/10.1136/archdischild-2016-310590
6. de Fatima Vasco Aragao M, van der Linden V, Brainer-Lima AM, Coeli RR, Rocha MA, Sobral da Silva P, Durce Costa Gomes de Carvalho M, van der Linden A et al (2016) Clinical features and neuroimaging (CT and MRI) findings in presumed Zika virus related congenital infection and microcephaly: retrospective case series study. BMJ 353:i1901. https://doi.org/10.1136/bmj.i1901
7. Dang J, Tiwari SK, Lichinchi G, Qin Y, Patil VS, Eroshkin AM, Rana TM (2016) Zika virus depletes neural progenitors in human cerebral organoids through activation of the innate immune receptor TLR3. Cell Stem Cell 19:258–265. https://doi.org/10.1016/j.stem.2016.04.014
8. Qian X, Nguyen HN, Song MM, Hadiono C, Ogden SC, Hammack C, Yao B, Hamersky GR et al (2016) Brain-region-specific organoids using mini-bioreactors for modeling ZIKV exposure. Cell 165:1238–1254. https://doi.org/10.1016/j.cell.2016.04.032
9. Garcez PP, Loiola EC, Madeiro da Costa R, Higa LM, Trindade P, Delvecchio R, Nascimento JM, Brindeiro R et al (2016) Zika virus impairs growth in human neurospheres and brain organoids. Science 352:816–818. https://doi.org/10.1126/science.aaf6116
10. Nowakowski TJ, Pollen AA, Di Lullo E, Sandoval-Espinosa C, Bershteyn M, Kriegstein AR (2016) Expression analysis highlights AXL as a candidate Zika virus entry receptor in neural stem cells. Cell Stem Cell 18:591–596. https://doi.org/10.1016/j.stem.2016.03.012
11. Tang H, Hammack C, Ogden SC, Wen Z, Qian X, Li Y, Yao B, Shin J et al (2016) Zika virus infects human cortical neural progenitors and attenuates their growth. Cell Stem Cell 18:587–590. https://doi.org/10.1016/j.stem.2016.02.016
12. Cugola FR, Fernandes IR, Russo FB, Freitas BC, Dias JL, Guimaraes KP, Benazzato C, Almeida N et al (2016) The Brazilian Zika virus strain causes birth defects in experimental models. Nature 534:267–271. https://doi.org/10.1038/nature18296
13. Hanners NW, Eitson JL, Usui N, Richardson RB, Wexler EM, Konopka G, Schoggins JW (2016) Western Zika virus in human

fetal neural progenitors persists long term with partial cytopathic and limited immunogenic effects. Cell Rep 15:2315–2322. https://doi.org/10.1016/j.celrep.2016.05.075
14. Gabriel E, Ramani A, Karow U, Gottardo M, Natarajan K, Gooi LM, Goranci-Buzhala G, Krut O et al (2017) Recent Zika virus isolates induce premature differentiation of neural progenitors in human brain Organoids. Cell Stem Cell 20:397–406 e5. https://doi.org/10.1016/j.stem.2016.12.005
15. Li C, Xu D, Ye Q, Hong S, Jiang Y, Liu X, Zhang N, Shi L et al (2016) Zika virus disrupts neural progenitor development and leads to microcephaly in mice. Cell Stem Cell 19:120–126. https://doi.org/10.1016/j.stem.2016.04.017
16. Wu KY, Zuo GL, Li XF, Ye Q, Deng YQ, Huang XY, Cao WC, Qin CF et al (2016) Vertical transmission of Zika virus targeting the radial glial cells affects cortex development of offspring mice. Cell Res 26:645–654. https://doi.org/10.1038/cr.2016.58
17. Li H, Saucedo-Cuevas L, Regla-Nava JA, Chai G, Sheets N, Tang W, Terskikh AV, Shresta S et al (2016) Zika virus infects neural progenitors in the adult mouse brain and alters proliferation. Cell Stem Cell 19:593–598. https://doi.org/10.1016/j.stem.2016.08.005
18. Shao Q, Herrlinger S, Yang SL, Lai F, Moore JM, Brindley MA, Chen JF (2016) Zika virus infection disrupts neurovascular development and results in postnatal microcephaly with brain damage. Development 143:4127–4136. https://doi.org/10.1242/dev.143768
19. Zhou T, Tan L, Cederquist GY, Fan Y, Hartley BJ, Mukherjee S, Tomishima M, Brennand KJ et al (2017) High-content screening in hPSC-neural progenitors identifies drug candidates that inhibit Zika virus infection in fetal-like organoids and adult brain. Cell Stem Cell 21:274–283 e5. https://doi.org/10.1016/j.stem.2017.06.017
20. Watanabe M, Buth JE, Vishlaghi N, de la Torre-Ubieta L, Taxidis J, Khakh BS, Coppola G, Pearson CA et al (2017) Self-organized cerebral organoids with human-specific features predict effective drugs to combat Zika virus infection. Cell Rep 21:517–532. https://doi.org/10.1016/j.celrep.2017.09.047
21. Yuan L, Huang XY, Liu ZY, Zhang F, Zhu XL, Yu JY, Ji X, Xu YP et al (2017) A single mutation in the prM protein of Zika virus contributes to fetal microcephaly. Science 358:933–936. https://doi.org/10.1126/science.aam7120
22. Yoon KJ, Song G, Qian X, Pan J, Xu D, Rho HS, Kim NS, Habela C et al (2017) Zika-virus-encoded NS2A disrupts mammalian cortical neurogenesis by degrading adherens junction proteins. Cell Stem Cell 21:349–358 e6. https://doi.org/10.1016/j.stem.2017.07.014
23. Chavali PL, Stojic L, Meredith LW, Joseph N, Nahorski MS, Sanford TJ, Sweeney TR, Krishna BA et al (2017) Neurodevelopmental protein Musashi-1 interacts with the Zika genome and promotes viral replication. Science 357:83–88. https://doi.org/10.1126/science.aam9243
24. Onorati M, Li Z, Liu F, Sousa AM, Nakagawa N, Li M, Dell'Anno MT, Gulden FO et al (2016) Zika virus disrupts phospho-TBK1 localization and mitosis in human neuroepithelial stem cells and radial glia. Cell Rep 16:2576–2592. https://doi.org/10.1016/j.celrep.2016.08.038
25. Zhang F, Hammack C, Ogden SC, Cheng Y, Lee EM, Wen Z, Qian X, Nguyen HN et al (2016) Molecular signatures associated with ZIKV exposure in human cortical neural progenitors. Nucleic Acids Res 44:8610–8620. https://doi.org/10.1093/nar/gkw765
26. Volvert ML, Rogister F, Moonen G, Malgrange B, Nguyen L (2012) MicroRNAs tune cerebral cortical neurogenesis. Cell Death Differ 19:1573–1581
27. Bian S, Sun T (2011) Functions of noncoding RNAs in neural development and neurological diseases. Mol Neurobiol 44:359–373
28. Zhang H, Shykind B, Sun T (2013) Approaches to manipulating microRNAs in neurogenesis. Front Neurosci 6:196
29. Kawase-Koga Y, Otaegi G, Sun T (2009) Different timings of dicer deletion affect neurogenesis and gliogenesis in the developing mouse central nervous system. Dev Dyn 238:2800–2812
30. De Pietri Tonelli D, Pulvers JN, Haffner C, Murchison EP, Hannon GJ, Huttner WB (2008) miRNAs are essential for survival and differentiation of newborn neurons but not for expansion of neural progenitors during early neurogenesis in the mouse embryonic neocortex. Development 135:3911–3921
31. Kawase-Koga Y, Low R, Otaegi G, Pollock A, Deng H, Eisenhaber F, Maurer-Stroh S, Sun T (2010) RNAase-III enzyme dicer maintains signaling pathways for differentiation and survival in mouse cortical neural stem cells. J Cell Sci 123:586–594
32. Gorski JA, Talley T, Qiu M, Puelles L, Rubenstein JL, Jones KR (2002) Cortical excitatory neurons and glia, but not GABAergic neurons, are produced in the Emx1-expressing lineage. J Neurosci 22:6309–6314
33. Rakic P (2005) Less is more: progenitor death and cortical size. Nat Neurosci 8:981–982
34. Makeyev EV, Zhang J, Carrasco MA, Maniatis T (2007) The MicroRNA miR-124 promotes neuronal differentiation by triggering brain-specific alternative pre-mRNA splicing. Mol Cell 27:435–448
35. Englund C, Fink A, Lau C, Pham D, Daza RA, Bulfone A, Kowalczyk T, Hevner RF (2005) Pax6, Tbr2, and Tbr1 are expressed sequentially by radial glia, intermediate progenitor cells, and postmitotic neurons in developing neocortex. J Neurosci 25:247–251
36. Bian S, Hong J, Li Q, Schebelle L, Pollock A, Knauss JL, Garg V, Sun T (2013) MicroRNA cluster miR-17-92 regulates neural stem cell expansion and transition to intermediate progenitors in the developing mouse Neocortex. Cell Rep 3:1398–1406
37. Shi Y, Zhao X, Hsieh J, Wichterle H, Impey S, Banerjee S, Neveu P, Kosik KS (2010) MicroRNA regulation of neural stem cells and neurogenesis. J Neurosci 30:14931–14936
38. Bian S, Xu TL, Sun T (2013) Tuning the cell fate of neurons and glia by microRNAs. Curr Opin Neurobiol 23:928–934. https://doi.org/10.1016/j.conb.2013.08.002
39. Fineberg SK, Kosik KS, Davidson BL (2009) MicroRNAs potentiate neural development. Neuron 64:303–309
40. Leucht C, Stigloher C, Wizenmann A, Klafke R, Folchert A, Bally-Cuif L (2008) MicroRNA-9 directs late organizer activity of the midbrain-hindbrain boundary. Nat Neurosci 11:641–648
41. Coolen M, Thieffry D, Drivenes O, Becker TS, Bally-Cuif L (2012) miR-9 controls the timing of neurogenesis through the direct inhibition of antagonistic factors. Dev Cell 22:1052–1064
42. Bonev B, Pisco A, Papalopulu N (2011) MicroRNA-9 reveals regional diversity of neural progenitors along the anterior-posterior axis. Dev Cell 20:19–32
43. Otaegi G, Pollock A, Hong J, Sun T (2011) MicroRNA miR-9 modifies motor neuron columns by a tuning regulation of FoxP1 levels in developing spinal cords. J Neurosci 31:809–818
44. Luxenhofer G, Helmbrecht MS, Langhoff J, Giusti SA, Refojo D, Huber AB (2014) MicroRNA-9 promotes the switch from early-born to late-born motor neuron populations by regulating Onecut transcription factor expression. Dev Biol 386:358–370. https://doi.org/10.1016/j.ydbio.2013.12.023
45. Jung HJ, Coffinier C, Choe Y, Beigneux AP, Davies BS, Yang SH, Barnes RH 2nd, Hong J et al (2012) Regulation of prelamin A but not lamin C by miR-9, a brain-specific microRNA. Proc Natl Acad Sci U S A 109:E423–E431. https://doi.org/10.1073/pnas.1111780109
46. Shibata M, Kurokawa D, Nakao H, Ohmura T, Aizawa S (2008) MicroRNA-9 modulates Cajal-Retzius cell differentiation by suppressing Foxg1 expression in mouse medial pallium. J Neurosci 28:10415–10421

47. Shibata M, Nakao H, Kiyonari H, Abe T, Aizawa S (2011) MicroRNA-9 regulates neurogenesis in mouse telencephalon by targeting multiple transcription factors. J Neurosci 31:3407–3422
48. Clovis YM, Enard W, Marinaro F, Huttner WB, De Pietri Tonelli D (2012) Convergent repression of Foxp2 3'UTR by miR-9 and miR-132 in embryonic mouse neocortex: implications for radial migration of neurons. Development 139:3332–3342
49. Gao FB (2010) Context-dependent functions of specific microRNAs in neuronal development. Neural Dev 5:25
50. Coolen M, Katz S, Bally-Cuif L (2013) miR-9: a versatile regulator of neurogenesis. Front Cell Neurosci 7:220. https://doi.org/10.3389/fncel.2013.00220
51. Calvet G, Aguiar RS, Melo AS, Sampaio SA, de Filippis I, Fabri A, Araujo ES, de Sequeira PC et al (2016) Detection and sequencing of Zika virus from amniotic fluid of fetuses with microcephaly in Brazil: a case study. Lancet Infect Dis 16:653–660. https://doi.org/10.1016/S1473-3099(16)00095-5
52. Martines RB, Bhatnagar J, Keating MK, Silva-Flannery L, Muehlenbachs A, Gary J, Goldsmith C, Hale G et al (2016) Notes from the field: evidence of Zika virus infection in brain and placental tissues from two congenitally infected newborns and two fetal losses—Brazil, 2015. MMWR Morb Mortal Wkly Rep 65:159–160. https://doi.org/10.15585/mmwr.mm6506e1
53. Ventura CV, Maia M, Bravo-Filho V, Gois AL, Belfort R Jr (2016) Zika virus in Brazil and macular atrophy in a child with microcephaly. Lancet 387:228. https://doi.org/10.1016/S0140-6736(16)00006-4
54. Mlakar J, Korva M, Tul N, Popovic M, Poljsak-Prijatelj M, Mraz J, Kolenc M, Resman Rus K et al (2016) Zika virus associated with microcephaly. N Engl J Med 374:951–958. https://doi.org/10.1056/NEJMoa1600651
55. Liang Q, Luo Z, Zeng J, Chen W, Foo SS, Lee SA, Ge J, Wang S et al (2016) Zika virus NS4A and NS4B proteins deregulate Akt-mTOR signaling in human fetal neural stem cells to inhibit neurogenesis and induce autophagy. Cell Stem Cell 19:663–671. https://doi.org/10.1016/j.stem.2016.07.019
56. Lin LF, Doherty DH, Lile JD, Bektesh S, Collins F (1993) GDNF: a glial cell line-derived neurotrophic factor for midbrain dopaminergic neurons. Science 260:1130–1132
57. Oo TF, Kholodilov N, Burke RE (2003) Regulation of natural cell death in dopaminergic neurons of the substantia nigra by striatal glial cell line-derived neurotrophic factor in vivo. J Neurosci 23:5141–5148
58. Perrelet D, Ferri A, Liston P, Muzzin P, Korneluk RG, Kato AC (2002) IAPs are essential for GDNF-mediated neuroprotective effects in injured motor neurons in vivo. Nat Cell Biol 4:175–179. https://doi.org/10.1038/ncb751
59. Deng YQ, Zhang NN, Li XF, Wang YQ, Tian M, Qiu YF, Fan JW, Hao JN et al (2017) Intranasal infection and contact transmission of Zika virus in guinea pigs. Nat Commun 8:1648. https://doi.org/10.1038/s41467-017-01923-4
60. Hong J, Zhang H, Kawase-Koga Y, Sun T (2013) MicroRNA function is required for neurite outgrowth of mature neurons in the mouse postnatal cerebral cortex. Front Cell Neurosci 7:151
61. Saito T (2006) In vivo electroporation in the embryonic mouse central nervous system. Nat Protoc 1:1552–1558